H_3O^+/Cl^- Association in High-Temperature Aqueous Solutions over a Wide Range of State Conditions. A Direct Comparison between Simulation and Electrical Conductance Experiment

A. A. Chialvo,[†,‡,*] P. C. Ho,[†] D. A. Palmer,[†] M. S. Gruszkiewicz,[†] P. T. Cummings,[†,§] and J. M. Simonson[†]

Chemical Sciences Division, High-Temperature Aqueous Chemistry Group, Oak Ridge National Laboratory, Oak Ridge, Tennessee 37831-6110, Department of Chemical Engineering, University of Tennessee, Knoxville, Tennessee 37996-2200, and Departments of Chemical Engineering, Chemistry and Computer Science, University of Tennessee, Knoxville, Tennessee 37996-2200

Received: August 22, 2001; In Final Form: November 16, 2001

The radial profiles of the potential of mean force for the $H_3O^+\cdots Cl^-$ pair are determined by constraint molecular dynamics of infinitely dilute high-temperature HCl aqueous solutions over a wide range of state conditions. The ion-pair association constant are consequently calculated and compared with those obtained from the most accurate recent electrical conductance experiments [Ho, P. C.; Palmer, D. A.; Gruszkiewicz, M. S. *J. Phys. Chem. B* **2001**, *105*, 1260−1266] at corresponding states. Resulting equilibrium constants between contact and solvent-shared ion-pair configurations indicate that more than 97% of configurations are contact ion-pairs. The adequacy of some simple fully electrostatic models to represent ion-pair association behavior in high-temperature aqueous solutions is also discussed.

1. Introduction

A great deal of effort has gone into the development of experimental methods for the straightforward measurement of the thermophysical properties of aqueous electrolyte solutions at high temperatures and pressures. This has been dictated by the need for more accurate methods of characterization of hydrothermal solutions in many natural environments,[1−3] and industrial processes.[4,5] The outcome of this effort has been 2-fold: On one hand, it is a welcome growth in quantity and accuracy of the experimental results; on the other hand, it represents a significant modeling challenge.[6] The heart of the matter resides in the rapid decrease of the dielectric constant of water with increasing temperature, a condition that facilitates the formation of ion pairs[7,8] and renders traditional, fully dissociated-solute, approaches of little use. However, the explicit inclusion of solute speciation into the modeling (i.e., association models), especially for weakly associated solutes, requires a detailed knowledge of the identity of the associated species in solution and the corresponding association constants in the desired range of state conditions and compositions. A recent attempt to develop such a model has been presented and tested recently for dilute aqueous sodium chloride solutions at near critical conditions.[9]

Although the conductance behavior for alkali halides is rather well established,[10−13] the association behavior of HCl studied by calorimetric techniques,[6] electrical conductance,[14−18] and solubility measurements,[19−23] is less certain.[23,24] More precisely, the dissociation constants determined by solubility data[21−23] appear to be at odds with those from conductance measurements.[15,17,18,25] These discrepancies point to various factors, including the intrinsic limitations of solubility approaches,[26] the difficulties in the measurement of electric conductivity in low-density dilute aqueous systems,[27] and the likely existence of additional species not taken into consideration in the treatment of solubility data.[23]

In this work, we focus on the ion-pair association in model aqueous HCl solutions at high temperature over a wide range of state conditions. The study encompasses the molecular-based determination of the ion-pair association constant via potential of mean force calculations, based on the recently tested intermolecular Gertner−Hynes potential model for the dissociated HCl, which gave a reasonable representation of the association constant at near critical conditions.[28] This presentation is organized as follows. In Section 2, we briefly describe the simulation methodology for the determination of the potential of mean force, and the intermolecular potentials involved in this study. In Section 3, we comment on the electric conductance experiments and the method used to extract the association constants. In Section 4, we present the simulation results for the dielectric constant of pure water and the association constant over a wide range of state conditions, as well as the comparison between the predicted and the experimentally determined results. Finally, in Section 5, we wrap up with a discussion of some relevant findings.

2. Simulation Methodology and Intermolecular Models

The molecular-based interpretation of, and molecular simulation route to, association constants in aqueous solutions have been described in detail elsewhere.[29,30] The simulation targets the direct and accurate determination of the radial profiles of the infinitely dilute anion−cation potential of mean force (PMF), which subsequently is integrated over the system volume to

* To whom correspondence should be addressed. E-mail: chialvoaa@ornl.gov. Fax: 865-574-4961.

† Chemical Sciences Division, High-Temperature Aqueous Chemistry Group, Oak Ridge National Laboratory.

‡ Department of Chemical Engineering, University of Tennessee.

§ Departments of Chemical Engineering, Chemistry and Computer Science, University of Tennessee.

10.1021/jp013255n CCC: $22.00
Published on Web 01/31/2002

obtain the association constant (see eq 3 in ref 28) and the corresponding equilibrium constant between ion-pair configurations (see Appendix A). These PMF profiles are determined simultaneously by two different though equivalent approaches, namely, the 'blue moon ensemble',[31,32] and the 'constraint-force'[33] methods. This is made possible by the required constraint dynamics of the anion−cation pair in the 'blue moon ensemble', which also provides the instantaneous values for the Lagrange multiplier needed in the 'constraint force' method (compare eq 6 and 8 in Ref.[28]), and allows a quick check of internal consistency.

We perform the required constraint dynamics between the spherical (Cl^-) and the nonspherical ion (H_3O^+), by allowing rotation of the hydronium while keeping it at a fixed distance from the chloride ion, via a SHAKE routine[34] with the (force) F-representation of Gear's predictor-corrector.[35] For the rigid-body dynamics of water and hydronium under isothermal-isochoric conditions, we implement a quaternion approach for the rotational degrees of freedom.[36] In addition, to achieve isothermal conditions, we implement three independent Nosé thermostats for the translational degrees of freedom of water, the rotational degrees of freedom of water and hydronium, and the translational degrees of freedom of the ions in the constrained ion-pair, respectively. Finally, we apply a Gear predictor−corrector algorithm,[37] 5^{th} order for the integration of the translational motion and 4^{th} order for the integration of the rotational motion and Nosé's dynamical variables with a time-step of 1.0 fs.

All simulations were performed with 254 water molecules and the ion-pair, across five state conditions, $0.834 \le \rho_r \le 1.965$ and $0.963 \le T_r \le 1.055$, to match those of the most recent and accurate electrical conductance measurements.[18] The Ewald summation was used to account for the electrostatic interactions, with a convergence parameter $\alpha \approx 5.6/L$, where L is the box length, and $\mathbf{k}$ in the reciprocal space such that $k^2 \le 27$. For each constrained distance, the simulation was run about 200 picoseconds after equilibration. Then, the final configuration for each constrained distance was used as the start-up configuration for the equilibration of the subsequent run. In each constraint dynamics simulation, we determined the time averages of the ion−ion and solvent induced ion-pair contributions to the mean force, as well as the time average of the constraint force (Lagrange multiplier). These averages were obtained over 10 blocks of 20 picoseconds each, to assess the corresponding statistics.

In this study, water was modeled according to the SPC/E model[38] for which we know its critical point.[39] This condition allows us to make meaningful comparisons with experiments using corresponding states, and thus, to attenuate the impact of the model imperfections on the predicted behavior.

For the ion−water interactions, we used the Gertner−Hynes model,[40] based on ab initio calculations for the ions H_3O^+ and Cl^- in TIP4P model water. Because for all practical purposes, the TIP4P and the SPC/E water models describe essentially the same behavior of water at high temperature,[41,42] we did not perform any re-parametrization for the ion−water force fields. The hydronium was described by a nonplanar four-site rigid geometry with a bond length $l_{OH} = 1.009$ Å, an HOH angle of 108.5°. Electronic structure calculations in water clusters indicate that the contact ion pair (CIP) is not fully ionic but rather a fractionally ionic/covalent ion-pair.[43] The charges δ^- on $Cl^{\delta-}$ and δ^+ on $H^{\delta+}$ for the $Cl^{\delta-}\cdots HOH_2^{\delta+}$ ion-pair can be taken as linear combinations between those from the molecular to the fully ionic ion-pair, i.e., the partial charge on $Cl^{\delta-}$ is $\delta^- = -0.841e$ and that on $H^{\delta+}$ is $\delta^+ = 0.496e$. The remaining partial charges on the hydronium are $\delta^+ = 0.5109e$ on the hydrogens, and $\delta^- = -0.6769e$ on the oxygen, respectively. Thus, the ion−water interactions are represented by Lennard−Jones interactions between the water's oxygen and either the hydronium's oxygen or the chloride ion (see Table 1), plus the corresponding electrostatic interactions between all charged sites, i.e.

TABLE 1: Lennard−Jones Parameters for the Gertner-Hynes Model[a]

	$Cl^{\delta-}$	$H_3O^{\delta+}$
σ_{OX}(Å)	3.563	2.529
ϵ_{OX}/k (*K*)	248.3	2172.9

[a] *X* denotes the heavy atom.

$$\phi_{wi}(r_{wi}) = 4\epsilon_{wi}\left[\left(\frac{\sigma_{wi}}{r_{wi}}\right)^{12} - \left(\frac{\sigma_{wi}}{r_{wi}}\right)^{6}\right] + \sum_{\alpha,\beta}^{3,4}\frac{q_w^\alpha q_i^\beta}{r_{wi}^{\alpha\beta}} \qquad (1)$$

where the subscripts *w* and *i* refer to water and ion, respectively; α and β denote the corresponding charged sites.

3. Electrical Conductance Measurements

For more than 30 years, measurements of electrical conductance of aqueous electrolyte solutions were carried out at ORNL using a static cell to handle high pressures and temperatures to 400 MPa and 1000 K, respectively.[10,44,45] Despite the success of these experiments, the static design still suffers from limited accuracy at low (near and sub-critical) densities, due to high solvent conductance and the inherently large temperature gradient along the vertical axis of the cell. In addition, the long residence time of the solution in the cell (which increases the likelihood of corrosion effects[15]) coupled to the above-mentioned effects limit the reliable range of measurement to electrolyte concentrations larger than $10^{-3}m$. These features prevent the use of the static cell for moderately weak electrolytes at high temperature;[11] therefore, a new flow-through cell was built to provide accurate measurements to concentrations as low as $10^{-7}m$.[27,46]

The experimental procedure was described in detail by Ho et al.[27,46] and will not be repeated here. Association constants were determined from the measured molar conductance by regression of the FHFP(Fuoss−Hsia−Fernandez−Prini) equation for the molar conductance and the mass action law,[47] i.e.

$$\Lambda = \alpha[\Lambda^\infty - S(\alpha c)^{0.5} - E\alpha c \ln(\alpha c) + J_1(a)\alpha c + J_2(a)(\alpha c)^{1.5}] \qquad (2)$$

$$K_a(M) = \rho^{-1}K_a(m) = (1-\alpha)/c(\alpha\gamma_\pm)^2 \qquad (3)$$

The degree of dissociation α, may be calculated by assuming the mean activity coefficient of the free ions given by the Debye−Hückel limiting law, i.e.

$$\ln\gamma_\pm = -\kappa q\alpha^{0.5}/(1+\kappa a\alpha^{0.5}) \qquad (4)$$

In these expressions, κ is the reciprocal radius of the ionic atmosphere, q is the Bjerrum distance ($q = e^2|z_-z_+|/(2kT\epsilon)$), where z denotes the ion charge, ϵ is the solvent's dielectric constant), a is the distance of closest approach, and M denotes molarity as opposed to m which indicates molality. Moreover, S is the slope of the Debye−Onsager limiting law, E, $J_1(a)$, and $J_2(a)$ are constants that depend on Λ^∞ and the solvent properties (viscosity and dielectric constant). Therefore, the

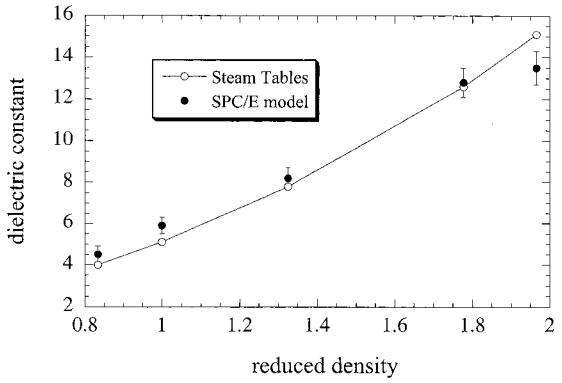

Figure 1. Comparison between tabulated and simulated (SPC/E model) dielectric constant of water at the five state conditions used in this investigation.

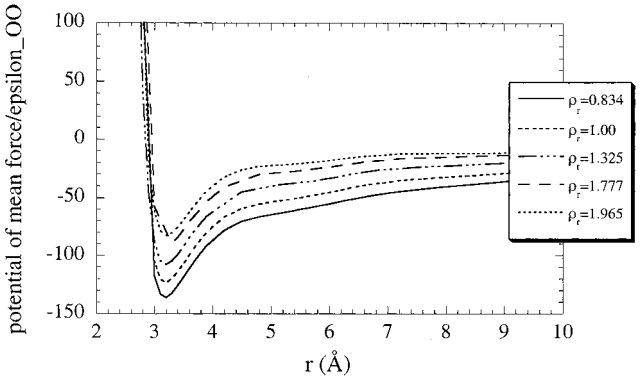

Figure 2. Comparison between the radial profiles of the $Cl^- - H_3O^+$ potential of mean force at the five state conditions used in this investigation. Potentials in units of $\epsilon_{SPC/E}$.

regression of the conductance data according to eqs 2−4 becomes just the least-squares adjustment of the mentioned parameters $J_1(a)$, $J_2(a)$, K_a (or α) and Λ^{∞}[48] according to the expression

$$\Lambda = \frac{\Lambda^{\infty} - S(\alpha c)^{0.5} + E\alpha c \ln(\alpha c) + J_1(a)\alpha c + J_2(a)(\alpha c)^{1.5}}{1 + \alpha c\, K_a \exp[-2\kappa q \alpha^{0.5}/(1 + \kappa a \alpha^{0.5})]} \quad (5)$$

A full account of the electrical conductance raw data and regressed quantities is given in Tables 1-2 of Ho et al.[18]

4. Simulation Results

In Figure 1 we compare the dielectric constant of the SPC/E water at the state conditions of this study with the corresponding tabulated experimental data.[49] The dielectric constant is used in the determination of the reference PMF, where it becomes approximately equal to the ion pair dielectrically screened electrostatic potential.[28] Note that the SPC/E model over-predicts the dielectric constant over the entire density range, except at the highest density. The maximum deviation between experimental and simulated values is about 10%.

In Figure 2 we compare the resulting profiles for the potentials of mean force, where the main feature is the distance and stability of the contact ion-pair (CIP) configuration. The first valley of this radial profile locates the CIP configuration around $r \approx 3.2$ Å, which appears to be independent of the state conditions over the range investigated. The stability of this ion-pair configuration, represented here by the depth of the valley (or conversely, the height of the corresponding radial distribution function), exhibits a rather strong dependence with state conditions, namely, the strength of the CIP configuration decreases with increasing density and temperature. Note however that there is a relatively weak formation of a solvent-shared ion-pair (SSHIP) configuration, in the form of an inflection point around 5.1Å < r < 5.6Å, which translates into a wide shoulder in the corresponding ion-pair radial distribution function.

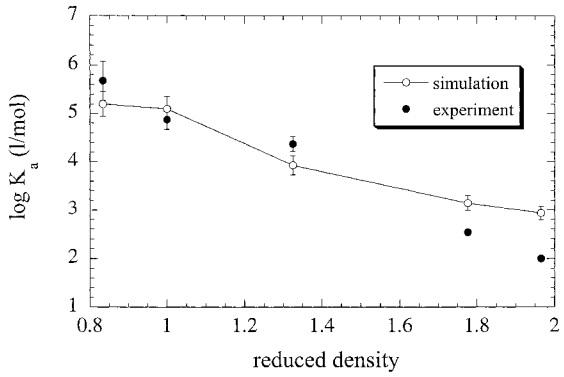

Figure 3. Comparison between the molecular-based predicted constant of association and the latest experimental values based on conductance measurements.

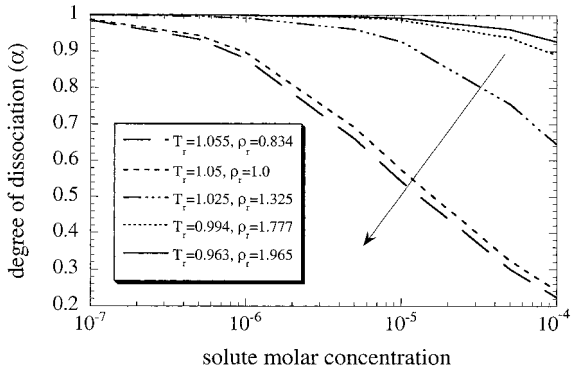

Figure 4. Predicted composition dependence of the degree of dissociation at the five state conditions used in this investigation.

The comparison between the constant of association from simulation and electrical conductance, Figure 3, indicates remarkable agreement especially for near-critical conditions, where they are within the combined uncertainties of simulation and experiment. Note also, this agreement deteriorates rather quickly as the system becomes denser (just in the region where electrical conductance data become more reliable).

In Figure 4 we display the calculated degree of dissociation from the predicted association constants within the concentration range where we can assume unit activity coefficients (see Appendix in ref 50). The most obvious feature is the large density effect on the degree of dissociation α at constant electrolyte concentration c_o. For example, at $c_o = 10^{-5}$ M α increases from 0.53 to 0.99 as the water density increases from $\rho_r = 0.834$ to $\rho_r = 1.965$. The density effect is slightly moderated by an opposite temperature effect,[50] even though here the range of temperature is rather smaller than the corresponding density range.

Because the profiles of PMF, and the corresponding radial distribution functions (RDF), do not exhibit a clear-cut resolution for the end of the first valley (first peak of the RDF), we assumed that location to be at $r \approx 3.9$Å. This choice allows us tentatively to assess the contribution of the SSHIP configuration to the association constant, in terms of the constant of equilibrium between the CIP and the SSHIP configurations (see Appendix A), and consequently, to estimate the percentage of

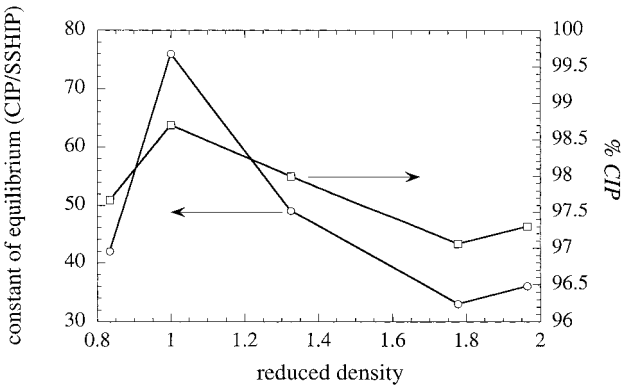

Figure 5. Molecular-based predicted constant of equilibrium between the CIP and the SSHIP configurations and the corresponding CIP population.

ion-pairs in each configuration. The estimated values of the corresponding constant of equilibrium between CIP and SSHIP are shown in Figure 5 together with the percentage of ion-pairs in the CIP configuration. This picture suggests that the ion-pair formation at these extreme conditions is dominated by contact ion-pairs (~97%); the distribution appears to be very weakly dependent on state conditions (except for a clear weak maximum at near criticality).

5. Discussion and Final Remarks

The constant of association calculations, based on the predicted PMF's, indicate that HCl behaves as a moderate to strong electrolyte in dilute aqueous solutions at near critical temperatures over a wide range of densities (Figure 4). In other words, at these conditions where water exhibits a rather small dielectric constant ($4 < \epsilon < 20$, see Figure 1) water is still able to screen the ion electrostatic interactions and to hinder the formation of ion pairs. This ability decreases dramatically for densities below the critical density of water and increasing HCl concentration, due to a combination of dielectric screening and ionic strength effects.

The comparison between electrical conductance and simulation results suggests a few questions and highlights worth addressing. The most obvious question concerns the observed departure of the predicted association constants from their experimental counterparts. To answer this question, we must first analyze the magnitude and nature of the uncertainties involved in our calculations. From the molecular simulation side, the most obvious sources of uncertainties have been discussed in some detail elsewhere.[50] In particular, the reference PMF contributes a distance-independent term in the integral defining the constant of association, i.e.

$$K_a = 4\pi\mathcal{R}\exp(e^2/\epsilon r_0 kT)\int_0^{r_o}\exp(-\int_{r_0}^{r} f_{AC}(r')dr')r^2dr \quad (6)$$

where $f_{AC}(r)$ denotes the radial profiles of the mean force obtained directly from the molecular dynamics simulations, and $\mathcal{R}$ is a numerical constant to obtain the association constant in the desired units. Because the dielectric constant and the temperature appear as absolute (as opposed to 'reduced') quantities, any uncertainty in these quantities will affect K_a exponentially through the pre-factor of the integral in eq 6. The uncertainties will most probably arise from the "imperfect" description of the vapor−liquid-phase envelope (critical conditions) by the water model. To assess the magnitude of this effect we analyze the pre-factors when the property values are those of the real water as opposed to those of the model water. This

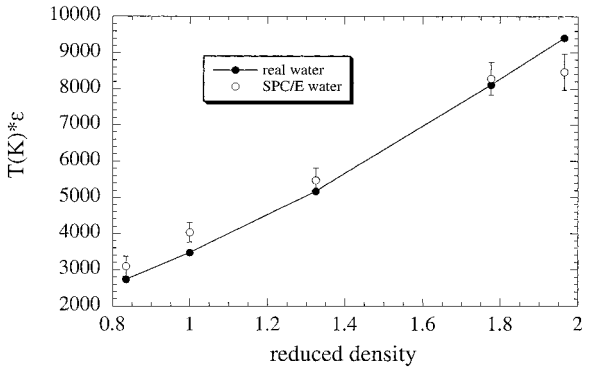

Figure 6. Comparison between the actual and the simulated (SPC/E) behavior of the product $\epsilon T(K)$.

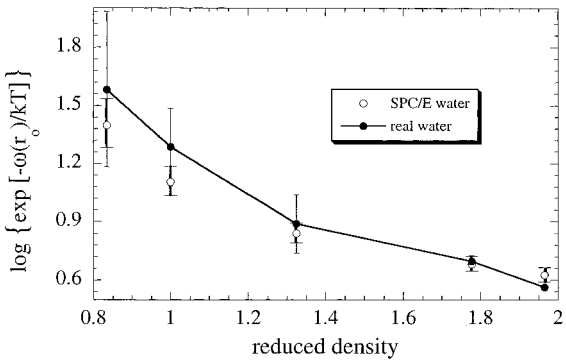

Figure 7. Comparison between the actual and the simulated (SPC/E) behavior of the reference potential of mean force, i.e., $\log\{\exp[-\omega(r_o)/kT]\}$.

is done in Figure 6 where we plot the product of the real temperature and the dielectric constant as a function of the reduced density. Note that, with the exception of the case for the highest density, the product $\epsilon T(K)$ for the real water is within the simulation uncertainties of the properties of the model water, i.e., $(\epsilon T(K))_{water} \cong (\epsilon T(K)_{SPC/E}$. This result would indicate that, regardless of the imperfection in either the VLE or the dielectric representation by the SPC/E water model, its effect on the reference PMF, and consequently, on the predicted K_a might be unimportant. In fact, we could turn this analysis all the way around and compare the logarithm of the exponential pre-factor $\log[\exp(e^2/kr_o\epsilon T)]$ for the SPC/E against that for real water. In Figure 7 we display this comparison where we include explicitly not only the uncertainties associated with the SPC/E dielectric constants but also, those associated with $\log K_a$ from the electrical conductance measurements. Note that, the error bars in the data for real water coming from $\log[\exp(e^2/kr_o\epsilon T)]$ are by far larger than those coming from $\log K_a$. This clearly suggests that the main source of discrepancy between simulation and experimental values of $\log K_a$ comes from the mean force portion of the calculation, i.e., from the exponential in the integrand of eq 6. In other words, the discrepancies are not so much related to the imperfections of the SPC/E model as to that of the ion−water parametrization. In summary, our results suggests that the models describe remarkably well the $H_3O^+\cdots Cl^-$ ion-pair association, if we consider that the intermolecular potential models were parametrized to properties unrelated to the phenomenon under study at ambient conditions. Moreover, regardless of the high accuracy of the conductance raw data, the association constants (or the corresponding degree of dissociation) must be estimated indirectly through less rigorous expressions which relate Λ, and the corresponding limiting

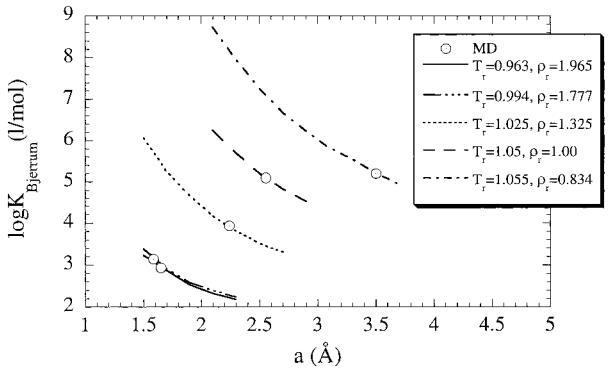

Figure 8. Predicted dependence of the log K_{Bjerrum} on the distance a of closest approach. The circles indicate the required distance for Bjerrum's model to predict the simulated association constants.

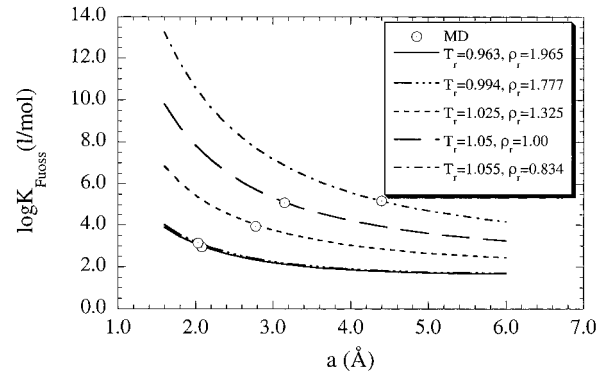

Figure 9. Predicted dependence of the logK_{Fuoss} on the distance a of closest approach. The circles indicate the required distance for Fuoss' model to predict the simulated association constants.

equivalent conductance Λ^∞ (see discussions by Fuoss,[51] Ibuki et al.,[52] and Barthel[53]).

A less obvious question regards the accuracy of some traditional ion association theories including Bjerrum's,[54] Fuoss',[55] and Prue's[56] (see Appendix B). Because we deal with precisely defined intermolecular potential models, our simulation results allow us to test unambiguously the adequacy of the traditional formalisms to describe ion pair formation. In Figures 8 and 9, we display the dependence of logK_a on the distance of closest approach (a) as predicted by Bjerrum and Fuoss expressions. In these pictures, we indicate the a values at which these models would predict the values of the constant of association found by PMF calculations. A simple comparison between the resulting values for a and the location of the first minimum in the PMF profiles (Figure 2) suggests that these 'fully electrostatic' models fail dramatically to describe adequately the ion-pair association of HCl at the conditions studied here. Obviously, the only way to find agreement between simulation and the Bjerrum and Fuoss models is to allow an unrealistic variation in the distance a with state conditions. The most obvious reason for such a failure is the missing nonelectrostatic contribution to the actual potential of mean force, which arise from the short-range ion−ion and ion−solvent interactions.

Acknowledgment. This research was sponsored by the Division of Chemical Sciences, Geosciences, and Biosciences, Office of Basic Energy Sciences, and by the Environmental Management Science Program (TTP OR17-SP22), under Contract No. DE-AC05-00OR22725 with Oak Ridge National Laboratory, managed and operated by UT-Battelle, LLC. P.T.C. was supported by the Division of Chemical Sciences, Geosciences, and Biosciences, Office of Basic Energy Sciences, U.S. Department of Energy.

Appendix A: Equilibrium Constant between CIP and SSHIP Configurations

Let assume that the free ions (FI), *i.e.,* anions and a cations are in equilibrium with two ion-pair configurations, such as the solvent-shared (SSHIP) and the contact (CIP) ion-pair configurations as indicated in the expression below

$$\text{FI} \overset{K_1}{\rightleftharpoons} \text{SSHIP} \overset{K_2}{\rightleftharpoons} \text{CIP} \tag{A1}$$

A simple species balance indicates that

$$[\text{SSHIP}] = c_o\beta_1(1-\beta_2)$$

$$[\text{CIP}] = c_o\beta_1\beta_2$$

$$[\text{SSHIP} + \text{CIP}] = c_o\beta_1 \tag{A2}$$

$$[\text{A}^-] = [\text{C}^+] = c_o(1-\beta_1)$$

where $[\cdots]$ denotes concentration, c_o is the initial electrolyte concentration, β_i are the degrees of advances of the corresponding equilibrium steps. Thus, according to the mass action law the two equilibrium constants become

$$K_1 = \beta_1(1-\beta_2)/c_o(1-\beta_1)^2 \tag{A3}$$

$$K_2 = \beta_2/(1-\beta_2) \tag{A4}$$

Thus, the association constant reads

$$K_a = \beta_1/[c_o(1-\beta_1)^2] \tag{A5}$$

where $\beta_1 = 1 - \alpha$ is the degree of ion-pair association, and $100\beta_2$ is the percentage of ion-pairs in the form of CIP configurations. From a microscopic viewpoint, K_2 can be written as

$$K_2 = \frac{[\text{CIP}]}{[\text{SSHIP}]} = \frac{\int_0^{r_1}\exp[-\omega(r)/kT]r^2dr}{\int_{r_1}^{r_o}\exp[-\omega(r)/kT]r^2dr} \tag{A6}$$

where $\omega(r) = -kT \ln g^{\infty}_{H_3O-Cl}(r)$ is the profile of the PMF, $r_1 \approx 3.9$Å is the location of the end of the first peak of $g^{\infty}_{H_3O-Cl}(r)$, and r_o is the (largest) distance at which we define the reference PMF.

Appendix B: 'Chemical Model at Low Concentration' and the 'Fully Electrostatic' Models

From very early in the development of the ion association theories, and despite their successful applications, there was some consensus about the limitations of the 'fully electrostatic' approaches.[57] These limitations are associated with the dielectric behavior of the solvent, assumed to be uniform and unaffected by the presence of the ion pair, and with the lack of any type of short-range (ion-pair and ion−solvent) interactions. Permittivity measurements suggest that the solvent dielectric constant is strongly modified in the neighborhood of the ions because the ions interact with each other and with the surrounding solvent.[58] These effects are highly sensitive to small perturbations of the ion-pair distance, and consequently, the use of 'fully electrostatic' models might result in unrealistic values for the

parameters (such as the 'contact' distance a) or the predicted association constants. To account for these important short-range interactions Barthel[59] developed a semi-phenomenological approach (low concentration Chemical Model, lcCM), by introducing a simple step function type potential $W^*_\pm$ for short-range contribution to the total PMF, i.e.

$$K_{\mathrm{lcCM}} = 4\pi\mathscr{R}\exp(-W^*_\pm/kT)\int_a^R r^2\exp(2q/r)dr \quad \text{(B1)}$$

where now a is taken from crystallographic data (as opposed to being an adjustable parameter), and $q = z_+z_-e^2/2\epsilon kT$ is the so-called Bjerrum's parameter. The regression of the electrical conductance measurements according to eqs 2−3, with $J_1(a)$ and $J_2(a)$ replaced by $J_1(R)$ and $J_2(R)$, respectively, and the Debye−Huckel limiting expression written as $\ln\gamma_\pm = kq\alpha^{0.5}/(1 + \kappa R\alpha^{0.5})$, allows us to obtain R, $W^*_\pm$, Λ_o, and therefore, $J_1(a)$, $J_2(a)$, and K_{lcCM} (or α).

Note that B1 is a rather general expression that includes several more restricted models. For example, if we set $W^*_\pm = 0$ in B1 we obtain Prue's[56] expression for the association constant. If we also set $R = q$ we obtain Bjerrum's expression (for details see eq 3.158 in § 3.8 of Bockris and Reddy[54]), written here in the traditional notation, i.e.

$$K_{\mathrm{Bjerrum}} = 4\pi\mathscr{R}a^3b^3\int_2^b y^{-4}\exp(y)dy \quad \text{(B2)}$$

where $y = 2q/r$ and $b = 2q/a$. Alternatively, if we set $W^*_\pm = 0$ and $R = 4a/3$ we have that $2q/r \approx b$ for $a \le r \le 4a/3$, and thus B1 reduces to Fuoss's expression,[55] i.e.

$$K_{\mathrm{Fuoss}} = (4\pi\mathscr{R}a^3/3)\exp(b) \quad \text{(B3)}$$

Note also that, the comparison between the lcCM expression for the constant of association and the corresponding PMF-based expression suggests the following relation

$$(2kTq/r) - W^*_\pm = \omega(r) \equiv PMF \quad \text{(B4)}$$

References and Notes

(1) *Geochemistry of Hydrothermal Ore Deposits*; 3rd ed.; Barnes, H. L., Ed.; John Wiley & Sons: New York, 1997.
(2) DeRonde, C. E. J.; Channer, D. M. D.; Faure, K.; Bray, C. J.; Spooner, E. T. C. *Geochim. Cosmochim. Acta* **1997**, *61*, 4025.
(3) Piccoli, P. M.; Candela, P. A.; Williams, T. J. *Lithos* **1999**, *46*, 591.
(4) Tester, J. W.; Cline, J. A. *Corrosion* **1999**, *55*, 1088.
(5) Fang, Z.; Xu, S. K.; Kozinski, J. A. *Ind. Eng. Chem. Res.* **2000**, *39*, 4536.
(6) Simonson, J. M.; Holmes, H. F.; Busey, R. H.; Mesmer, R. E.; Archer, D. G.; Wood, R. H. *J. Phys. Chem.* **1990**, *94*, 7675.
(7) Pitzer, K. S. *Phys. Chem. Earth* **1981**, *13/14*, 175.
(8) Gilkerson, W. R. *J. Phys. Chem.* **1970**, *74*, 746.
(9) Oscarson, J. L.; Palmer, B. A.; Fuangswasdi, S.; Izatt, R. M. *Ind. Eng. Chem. Res.* **2001**, *40*, 2176.
(10) Ho, P. C.; Palmer, D. A.; Mesmer, R. E. *J. Sol. Chem.* **1994**, *23*, 997.
(11) Zimmerman G. H.; Gruszkiewicz, M. S.; Wood, R. H. *J. Phys. Chem.* **1995**, *99*, 11 612.
(12) Gruszkiewicz, M. S.; Wood, R. H. *J. Phys. Chem. B* **1997**, *101*, 6549.
(13) Ho, P. C.; Palmer, D. A. *J. Chem. Eng. Data* **1998**, *43*, 102.
(14) Noyes, A. A. *The Electrical Conductivity of Aqueous Solutions*; Carnegie Institution of Washington: Washington, D.C., 1907; Vol. Publication #63.
(15) Franck, E. U. *Zietschr. Phys. Chemie N. F.* **1956**, *8*, 192.
(16) Pearson, D.; Copeland, C. S.; Benson, S. W. *J. Am. Chem. Soc.* **1963**, *85*, 1047.
(17) Frantz, J. D.; Marshall, W. L. *Am. J. Sci.* **1984**, *284*, 651.
(18) Ho, P. C.; Palmer, D. A.; Gruszkiewicz, M. S. *J. Phys. Chem. B* **2001**, *105*, 1260.
(19) Chou, I. M.; Frantz, J. D. *Am. J. Sci.* **1997**, *277*, 1067.
(20) Frantz, J. D.; Popp, R. K. *Geochim. Cosmochim. Acta* **1979**, *43*, 1223.
(21) Ruaya, J. R.; Seward, T. M. *Geochim. Cosmochim. Acta* **1987**, *51*, 121.
(22) Sverjensky, D. A.; Hemley, J. J.; D'Angelo, W. M. *Geochim. Cosmochim. Acta* **1991**, *55*, 989.
(23) Tagirov, B. R.; Zotov, A. V.; Akinfiev, N. N. *Geochim. Cosmochim. Acta* **1997**, *61*, 4267.
(24) Pokrovskii, V. *Geochim. Cosmochim. Acta* **1999**, *63*, 1107.
(25) Lukashow, Y. M.; Komissarov, K. B.; Golubev, S. N.; Svistunov, E. P. *Teploenergetika (English version)* **1975**, *22*, 78.
(26) Chialvo, A. A.; Driersner, T., Manuscript in preparation, 2002.
(27) Ho, P. C.; Bianchi, H.; Palmer, D. A.; Wood, R. H. *J. Sol. Chem.* **2000**, *29*, 217.
(28) Chialvo, A. A.; Cummings, P. T.; Simonson, J. M. *J. Chem. Phys.* **2000**, *113*, 8093.
(29) Chialvo, A. A.; Cummings, P. T. Supercritical Water and Aqueous Solutions: Molecular Simulation. In *Encyclopedia of Computational Chemistry*; Scheyer, P. v. R., Ed.; Wiley & Sons: 1998; Vol. 4; p 2839.
(30) Chialvo, A. A.; Cummings, P. T.; Cochran, H. D.; Simonson, J. M.; Mesmer, R. E. *J. Chem. Phys.* **1995**, *103*, 9379.
(31) Carter, E. A.; Ciccotti, G.; Hynes, J. T.; Kapral, R. *Chem. Phys. Lett.* **1989**, *156*, 472.
(32) Ciccotti, G.; Ferrario, M.; Hynes, J. T.; Kapral, R. *Chem. Phys.* **1989**, *129*, 241.
(33) Sprik, M.; Ciccotti, G. *J. Chem. Phys.* **1998**, *109*, 7737.
(34) Ciccotti, G.; Rychaert, J. P. *Comp. Phys. Rep.* **1986**, *4*, 345.
(35) van Gunsteren, W. F.; Berensen, H. J. C. *Mole. Phys.* **1997**, *34*, 1311.
(36) Evans, D. J.; Murad, S. *Mole. Phys.* **1997**, *34*, 327.
(37) Gear, C. W. "The Numerical Integration of Ordinary Differential Equations of Various Orders," Argonne National Laboratory, 1966.
(38) Berendsen, H. J. C.; Grigera, J. R.; Straatsma, T. P. *J. Phys. Chem.* **1987**, *81*, 6269.
(39) Guissani, Y.; Guillot, B. J. *J. Chem. Phys.* **1993**, *98*, 8221.
(40) Gertner, B. J.; Hynes, J. T. *Faraday Discussions* **1998**, *110*, 301.
(41) Chialvo, A. A.; Cummings, P. T. *J. Phys. Chem.* **1996**, *100*, 1309.
(42) Chialvo, A. A.; Cummings, P. T. Molecular-based Modeling of Water and Aqueous Solutions at Supercritical Conditions. In *Advances in Chemical Physics*; Rice, S. A., Ed.; Wiley & Sons: New York, 1999; Vol. 109; p 115.
(43) Ando, K.; Hynes, J. T. *J. Phys. Chem. B* **1997**, *101*, 10464.
(44) Quist, A. S.; Marshall, W. L. *J. Phys. Chem.* **1968**, *72*, 684.
(45) Mesmer, R. E.; Marshall, W. L.; Palmer, D. A.; Simonson, J. M.; Holmes, H. F. *J. Sol. Chem.* **1988**, *17*, 699.
(46) Ho, P. C.; Palmer, D. A.; Wood, R. H. *J. Phys. Chem. B* **2000**, *104*, 12084.
(47) Fernandez-Prini, R. *Trans. Faraday Soc.* **1969**, *65*, 3311.
(48) Barthel, J. M. G.; Krienke, H.; Kunz, W. *Physical Chemistry of Electrolyte Solutions*; Springer: Darmstadt, 1998; Vol. 5.
(49) Haar, L.; Gallagher, J. S.; Kell, G. S. *Steam Tables*; Hemisphere Publishing Corporation: New York, 1984.
(50) Chialvo, A. A.; Cummings, P. T.; Simonson, J. M.; Mesmer, R. E. *J. Chem. Phys.* **1996**, *105*, 9248.
(51) Fuoss, R. M. *J. Phys. Chem.* **1974**, *78*, 1383.
(52) Ibuki, K.; Ueno, M.; Nakahara, M. *J. Phys. Chem. B* **2000**, *104*, 5139.
(53) Barthel, J. *Pure Appl. Chem.* **1979**, *51*, 2093.
(54) Bockris, J. O. M.; Reddy, A. K. N. *Modern Electrochem.*; Plenum Press: New York, 1998; Vol. 1.
(55) Fuoss, R. M. *J. Am. Chem. Soc.* **1958**, *80*, 5059.
(56) Prue, J. E. *J. Chem. Ed.* **1969**, *46*, 12.
(57) Davies, C. W. *Ion Association*; Butterworth: Washington, 1962.
(58) Barthel, J.; Wachter, R.; Gores, H.-J. Temperature Dependence of Conductance of Electrolytes in Nonaqueous Solutions. In *Modern Aspects of Electrochemistry*; Conway, B. E., Bockris, J. O. M., Eds.; Plenum Press: New York, 1979; Vol. 13; p 1.
(59) Barthel, J. *Ber. Bunsen-Ges. Phys. Chem.* **1979**, *83*, 252.